Isoxazolo-[3,4-*d*]-pyridazin-7-(6*H*)-ones and their Corresponding 4,5-Disubstituted-3-(2*H*)-pyridazinone Analogues as New Substrates for α_1-Adrenoceptor Selective Antagonists: Synthesis, Modeling, and Binding Studies

Federica Montesano,[a] Daniela Barlocco,[a] Vittorio Dal Piaz,[b]
Amedeo Leonardi,[c] Elena Poggesi,[c] Francesca Fanelli[d]
and Piero G. De Benedetti[d],*

[a]*Ist. Chimica Farmaceutica e Tossicologica, Viale Abruzzi 42, 20131 Milano, Italy*
[b]*Dip. Scienze Farmaceutiche, Via G. Capponi, 9 - 50121 Firenze, Italy*
[c]*Pharmaceutical R&D Division, Recordati s.p.a., Via M. Civitali 1, 20148 Milano, Italy*
[d]*Dipartimento di Chimica, Via Campi 183, 41100 Modena, Italy*

Abstract—A series of phenylpiperazinylalkyl moieties were attached to monocyclic or bicyclic substituted pyridazinones and the new compounds tested for their affinity towards α_1-adrenoceptor and its α_{1a}, α_{1b} and α_{1d} subtypes, as well as serotonin 5-HT$_{1A}$ receptor. Several analogues (**5**, **6**, **9**, and **10**) showed remarkable potency and selectivity towards α_{1a}, and α_{1d} with respect to α_{1b} subtype. None of the test compounds exhibited significant affinity for 5-HT$_{1A}$ receptor. Finally, on the basis of the α_1-AR subtypes 3D models recently proposed, we have elaborated theoretical interaction models for the new compounds. The theoretical study allowed us to predict the affinity of the new compounds as well as to infer the structural/dynamics determinants of their interaction with the three α_1-AR subtypes. © 1998 Published by Elsevier Science Ltd. All rights reserved.

Introduction

α_1-Adrenergic receptors (α_1-AR) are members of the superfamily of G protein coupled receptors (GPCR) that transduce signal across the cell membrane. The α_1-ARs mediate the functional effects of catecholamines like epinephrine and norepinephrine by coupling to the Gq mediated activation of phospholipase C culminating into the phosphoinositide (PI) hydrolysis. The initial subdivision of the α_1-AR into subtypes was based primarily on the selectivity of WB-4101 for the α_1A-subtype[1] and the selective alkylation of the α_1B-subtype shown by chloroethylclonidine (CEC).[2] Other antagonists selective for the α_1A-AR were identified, such as 5-methylurapidil[3] and S-(+)-niguldipine.[4]

Molecular biology techniques allowed the identification of cDNAs encoding three α_1-ARs, namely the rat $\alpha_{1a/d}$, the hamster α_{1b} and the bovine α_{1c}.[5–9] Originally, the pharmacological characteristics of the cloned subtypes appeared to be inconsistent with the pharmacological properties of the native subtypes: the existence of four subtypes was also suggested.[9]

It is now clear that the three recombinant α_1-ARs correlate closely with the three α_1-AR subtypes that were identified in native tissues and which mediate their functional responses.[10–12] These receptors are now designated as α_{1A} (α_{1a}), α_{1B} (α_{1b}), and α_{1D} (α_{1d}), with lower case subscripts being used to designate the recombinant receptors, and upper case subscripts to denote the native receptors.[13] The recombinant receptor previously designated as α_{1c}-AR has now been shown to correspond to the native α_{1A}-AR,[10,14–16] and as such, the terms α_{1C}- or α_{1c}-AR are no longer used.[17]

Furthermore, the α_{1D}-AR has now been characterized in detail, and antagonists capable of discriminating between this receptor and the α_{1A}-AR are now available, confirming that these two receptors represent distinct α_1-AR subtypes.[18,19]

In addition to α_{1A}, α_{1B} and α_{1D}-AR subtypes, which share a high affinity for prazosin, the existence of additional α_1-AR has been proposed. These are called α_{1L}-ARs and are characterized by a low functional affinity for prazosin, intermediate affinity for WB 4101 and 5-methylurapidil and resistance to CEC alkylation.[20–22] The presence of these different α_1-AR subtypes in blood vessels and other smooth muscles points to the importance of developing selective drugs for receptor classification and characterization as well as for therapeutic effectiveness.

The understanding of the molecular determinants of drug selectivity towards GPCRs is a very challenging target. One obvious problem is our limited knowledge of the 3D structure of these membrane proteins, because of difficulties linked to their non degenerative purification and crystallization. Moreover, even if a highly resolved structure of a GPCR were immediately available, the description of the mechanism of ligand–receptor selective interaction in terms of both structure and dynamics would remain a daunting task. This problem may be approached by combining 3D model building of receptor structure and computational simulation of receptor dynamics. In this context, some of us recently presented a preliminary rationalization, at the molecular level, of antagonist selectivity towards the three cloned α_1-AR subtypes.[23] Molecular dynamics simulations allowed a structural/dynamics analysis of the three receptor structures in their free forms. This analysis was paralleled by docking simulations, using 16 selective and nonselective antagonists that provided theoretical quantitative structure–affinity relationship models.[23] This theoretical study led to the hypothesis that the transmembrane domains of the α_1-AR subtypes have different dynamic behaviors and different topographies of the binding sites, which are mainly constituted by conserved residues. In particular, the α_{1a}-AR binding site is more flexible and topographically different with respect to the other two subtypes. In other words, the nonconserved residues seemed to exert intramolecular rather than intermolecular effects, conferring different structural/dynamics features to the conserved ligand binding sites.

Amongst the compounds showing high affinity towards α_1-AR relevant attention has recently been devoted to a series of phenylpiperazines of general structure **I**, where Ar represents several aromatic residues nonstructurally related. Amongst others, the pyridazine system was investigated by some of us[24] as a possible substituent for piperazinyl derivatives. In the search of more potent and selective α_1-AR compounds, we have now synthesized and tested a new series in which a phenyl-piperazinylalkyl moiety has been introduced at different positions of the previously reported[25,26] 3,4-disubstituted-isoxazolo-[3,4-d]-pyridazin-7-(6H)-one (**1**) and of its open analogue **2**.

Moreover, on the basis of the α_1-AR 3D models recently proposed,[23] we have elaborated theoretical interaction models between the new compounds and the three α_1-AR subtypes. The theoretical study allowed us to predict the affinity of the new compounds as well as to infer the structural/dynamics determinants of their selective interaction with the three α_1-AR subtypes.

Chemistry

The 6-substituted isoxazolo-[3,4-d]-pyridazin-7-(6H)-ones (**5–7**) were prepared by alkylation of compound **1** by the required dibromoalkane in dimethylformamide and potassium carbonate at room temperature, followed by condensation with the appropriate substituted phenyl-piperazine in acetone and potassium carbonate at 80 °C. According to the same scheme, the corresponding open derivatives (**9–11**) were prepared, starting from **2** (see Scheme 1).

Alternatively, compounds **5–7** and **9–11** could be prepared by treatment with the required substituted-4-phenylpiperazin-1-yl-alkyl chloride, in turn obtained by condensation in acetone and potassium carbonate of the appropriate phenylpiperazine and the dihaloalkane[27] (see Scheme 1). No significantly different yields were obtained from the two pathways. The lower homologs **4** and **8** were obtained in good yields by Mannich reaction, starting from **1** and **2**, respectively (see Scheme 2).

Finally, the 3-substituted **12** was prepared by nucleophilic substitution on the 3-bromomethylisoxazolo-pyridazinone **3**[28] by ortho-methoxyphenylpiperazine in
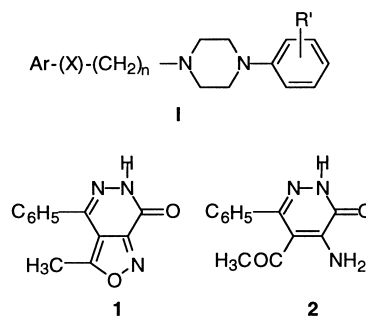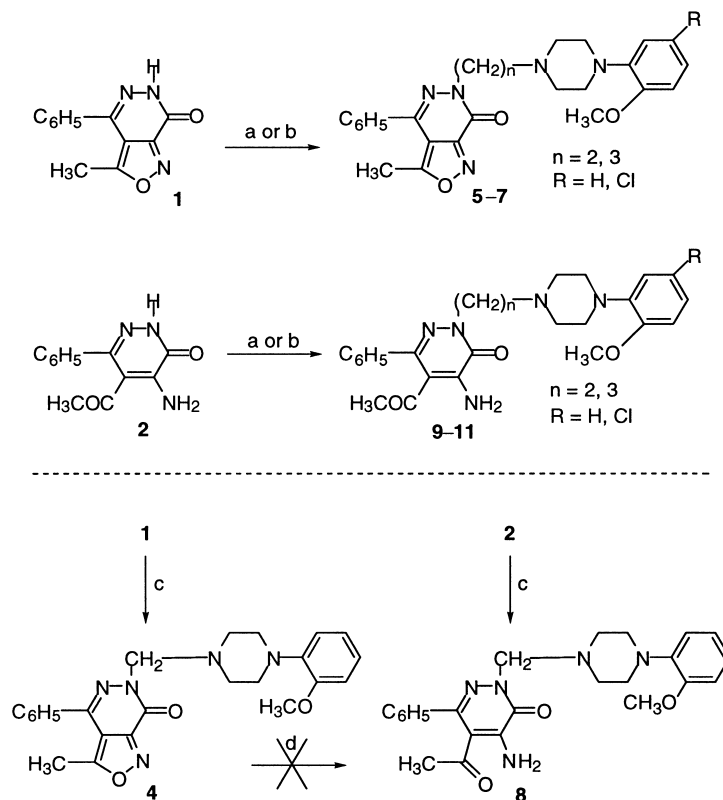

Chart 1.

Scheme 1. Reagents and conditions: (a) 1. Br(CH₂)nBr, DMF, K₂CO₃, rt, 2. [piperazine structure], K₂CO₃, Δ, acetone; (b) [Cl(CH₂)n piperazine structure], K₂CO₃, Δ acetone; (c) *ortho*-methoxyphenylpiperazine, HCHO, EtOH, Δ; (d) NH₂-NH₂·H₂O, 10% Pd-C, EtOH, Δ.

chloroform at 60 °C (Scheme 2). Treatment of **12** with hydrazine hydrate in refluxing ethanol in the presence of 10% Pd-C led to the open analogue **13** in 70% yield (Scheme 2). It should be noted that attempts to apply
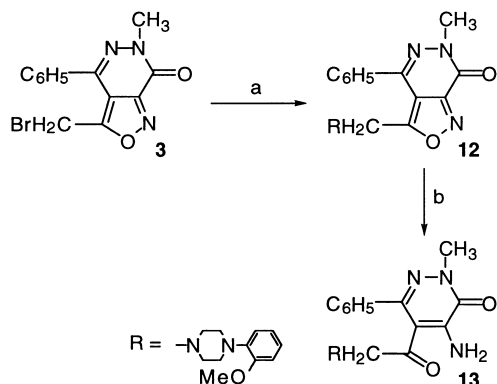
Scheme 2. Reagents and conditions: (a) *ortho*-methoxy-phenylpiperazine, CHCl₃, 60 °C; (b) NH₂-NH₂·H₂O, 10% Pd-C, EtOH, Δ.

the same reductive opening of the isoxazole ring to the above reported **4** always brought about a parallel loss of the alkylpiperazinyl moiety at position 6. See Experimental and Table 1 for the chemical and physical data of the newly synthesized compounds.

Binding studies

All compounds were tested for their affinity towards native α_1-receptor (^{3}H-prazosin as specific ligand on rat cerebral cortex), 5-HT$_{1A}$ receptor (^{3}H-8-OH-DPAT, rat hippocampus) and the cloned receptor subtypes expressed on CHO cells (^{3}H-prazosin). In case of good affinity for the α_{1d} subtype, additional testing on human recombinant α_{1a} and α_{1b} AR subtypes was performed. Prazosin, 8-OH-DPAT and BMY 7378 were used as reference standards. Data are shown in Table 2.

Modeling

The building of the 3D model of the three α_1-AR sub-types was described in detail in our previous paper.[23]

Table 1. Physicochemical data of compounds **4–11**
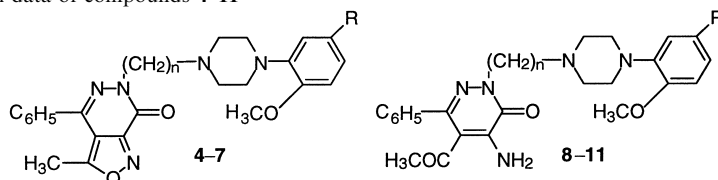
Compd	n	R	% Yield	mp (°C)	Formula
4	1	H	79	166–168	$C_{24}H_{25}N_5O_3$
5	2	H	70[a]	128–129	$C_{25}H_{27}N_5O_3$
6	2	Cl	72[a]	160–162	$C_{25}H_{26}ClN_5O_3$
7	3	Cl	68[b]	130–131	$C_{26}H_{28}ClN_5O_3$
8	1	H	51	198–200	$C_{24}H_{27}N_5O_3$
9	2	H	63[a]	154–155	$C_{25}H_{29}N_5$
10	2	Cl	70[b]	154–155	$C_{25}H_{28}ClN_5O_3$
11	3	H	65[b]	oil	$C_{26}H_{31}N_5O_3$

[a]Method B.
[b]Method A.

Table 2. Affinity constants (K_i, nM) of compounds **4–13** towards native α_1 and 5-HT$_{1A}$ receptors and cloned α_1 adrenoceptor subtypes

	K_i (nM), native receptors (rat brain)			K_i (nM), cloned receptors (human brain)		
Compd	α_1	5-HT$_{1A}$	Ratio 5-HT$_{1A}$/α_1	α_{1a}	α_{1b}	α_{1d}
4	2308	480.3	0.21	NT	NT	315.8
5	147.1	1101	7.48	1.49	31.09	1.53
6	15.57	2203	141.5	1.85	7.72	0.26
7	7.86	1434	182.4	1.55	2.57	1.32
8	2395	395.7	0.16	NT	NT	596.8
9	24.56	123.1	5.01	4.75	22.06	0.93
10	42.68	NT	NT	6.27	17.82	0.75
11	46.73	2868	61.37	18.81	142.9	137.8
13	515.6	NT	NT	NT	NT	84.74
prazosin	0.74	2357	3185	0.58	0.28	0.29
BMY7378	281.9	0.37	0.00	378.4	70.9	1.28
8-OH-DPAT	18002	2.33	0.00	NT	NT	NT

Equilibrium dissociation constants (K_i) were derived from IC$_{50}$ using the Cheng–Prusoff equation.[34] The affinity estimated were derived from displacement of [³H]prazosin binding for α_1-adrenoceptors and [³H]8-hydroxy-2-(di-n-propylamino)tetraline for 5-HT$_{1A}$ receptor. Each experiment was performed in triplicate. The lable NT means not tested.

The average minimized structures of the α_1-AR subtypes previously obtained were used for providing ligand-receptor interaction models for the new synthesized compounds. For each ligand–receptor minimized complex, an intermolecular interaction descriptor was computed and the linear regression equations previously presented were used to calculate the affinities of the new compounds for the three α_1-AR subtypes.

Results and Discussion

The most interesting compounds presented in this work (**5–7**, **9**, and **10**) carry an ethylenic or a propylenic chain as a spacer (see Table 2). These compounds show reasonable α_1-AR binding affinity values resulting from the different contribution of α_{1a} and α_{1b}-AR subtypes; moreover, they show low affinity for the 5-HT$_{1A}$ receptor. In general, 2-methoxy-5-chloro-phenylpiperazines show higher α_1/5-HT$_{1A}$ selectivity than the corresponding 2-methoxyphenylpiperazines.[29] None of compounds **4–13** showed significant potency towards 5-HT$_{1A}$, as clearly indicated by the results reported in Table 2. In particular, for the most potent α_1-antagonists in this series (**7**) the ratio between the two K_is approaches a value close to 200.

In order to better define the above trends, the molecular determinants of affinity and selectivity of the new

compounds towards the three α_1-AR subtypes have been investigated by means of a theoretical study of ligand–receptor interactions.

A theoretical intermolecular interaction descriptor as a predictor of the affinity/selectivity towards the three α_1-AR subtypes

Recently, some of us presented a theoretical investigation, at the molecular level, of antagonist selectivity towards the three cloned α_1-AR subtypes.[23] A quantitative description of the theoretical results, which were based on the structural/dynamics analysis of the free receptor forms, was provided by docking each of the antagonists into the average minimized structures of the three α_1-AR subtypes. For each selected ligand–receptor minimized complex the theoretical binding energies (BE) were computed and correlated with the experimental binding affinities (pK_i) measured on the three animal cloned subtypes; the resulting linear regression equations are reported as follows:

(a) $pK_{1a} = 5.45(\pm 0.37) - 0.08(\pm 0.01)BE_{1a}$, $n = 16$, $r = 0.90$, $s = 0.52$;

(b) $pK_{1b} = 4.20(\pm 0.32) - 0.12(\pm 0.01)BE_{1b}$, $n = 16$, $r = 0.94$, $s = 0.37$;

(c) $pK_{1d} = 4.43(\pm 0.36) - 0.09(\pm 0.01)BE_{1d}$, $n = 16$, $r = 0.92$, $s = 0.39$;

where n is the number of compounds, r is the correlation coefficient, s is the standard deviation and the number in parentheses give the 95% confidence intervals.

The BE of the ligand–receptor minimized complexes were computed according to the following formula: $BE = IE + ER + EL$, where IE is the ligand–receptor interaction energy and ER and EL are the distortion energies of the receptor and of the ligand, respectively, calculated as differences between the energies of the bound and of the free optimized molecular forms.

Receptor and ligand distortion energies provide a measure of both ligand and receptor penalties to go from the free to the bound state. In other words, the higher the receptor and ligand distortion energies the lower the ligand–receptor interaction propensity and, hence, the lower the ligand–receptor dynamic complementarity. From these studies it was concluded that, the 'theoretical α_{1a} selectivity', that is the selectivity encoded by theoretical descriptors, is mainly modulated by receptor and ligand distortion energies. In other words, subtype selectivity seemed to be mainly guided by dynamic complementarity (induced fit) between the ligand and the receptor.

In the present work, the average minimized structures of the α_1-AR subtypes previously obtained have been used for providing ligand–receptor interaction models for the new synthesized compounds. Each compound has been docked into the average minimized structures of the three α_1-AR subtypes following the docking criteria and the results of the previous theoretical study.[23] Moreover, for each ligand–receptor minimized complex, the BE have been computed and the linear regression equations previously presented (see above in the text) have been used for calculating the affinities of the new compounds. Table 3 shows the theoretical binding affinities as well as the theoretical intermolecular interaction descriptors computed on the ligand-receptor minimized complexes. Interestingly, the theoretical binding affinities (Table 3) interpolated from the previously reported linear regression models, calibrated on the animal cloned α_1-AR subtypes, are consistent with the experimental binding affinity data, measured towards the three human cloned α_1-AR subtypes (Table 2).

It can be seen that the generic α_1-AR affinities of compounds **5**, **6**, **9**, and **10** are quite increased if the affinity values towards the cloned α_{1a}- and α_{1d}-ARs are considered. This is mainly due to the fact that these compounds show a high affinity as well as a remarkable

Table 3. Computed binding affinities (K) and binding (BE, kcal/mol), interaction (IE, kcal/mol), receptor distortion (ER, kcal/mol), and ligand distortion (EL, kcal/mol) energies of the ligand-α_1-adrenoceptor subtype complexes

Compd	Kla	K1b	K1d	BE1a	IE1a	ER1a	EL1a	BE1b	IE1b	ER1b	EL1b	BE1d	IE1d	ER1d	EL1d
4			426.58									−21.62	−77.26	47.58	8.06
5	2.75	46.77	2.00	−38.88	−87.17	43.83	4.46	−26.11	−79.13	48.24	4.78	−47.78	−84.13	30.33	6.32
6	0.45	34.67	0.52	−48.80	−90.21	35.27	6.14	−27.21	−80.70	48.95	4.54	−53.85	−90.21	25.70	10.66
7	0.55	0.78	4.68	−47.58	−92.60	36.97	8.05	−40.91	−81.76	36.26	4.59	−43.43	−89.92	38.85	7.64
8			524.81									−20.56	−76.52	42.58	13.38
9	2.45	10.47	0.14	−39.55	−89.28	42.71	7.02	−31.60	−83.37	47.15	4.62	−60.27	−93.99	24.74	8.98
10	1.48	3.31	0.15	−42.28	−91.53	40.73	8.52	−35.65	−85.25	45.28	4.32	−59.87	−98.03	25.34	12.82
11	16.89	32.36	75.86	−28.95	−81.73	47.45	5.33	−27.44	−81.20	45.96	7.80	−21.91	−93.88	52.70	11.27
13			20.89									−36.12	−80.38	34.22	10.04

selectivity for these two α_1-AR subtypes than for the α_{1b}-AR subtype. Interestingly, the high affinity compounds **5**, **6**, **9**, and **10** show slight α_{1d}/α_{1a} and high α_{1d}/α_{1b} selectivities, suggesting that they can constitute good templates for designing high affinity and selective antagonists towards the α_{1d}-AR subtype. The importance of these compounds is remarkable considering the low number of available high affinity and selective antagonists for the α_{1d} or the α_{1b}.

By analysing the theoretical descriptors reported in Table 3 it can be inferred that low α_{1d} binding energies (high affinity) are reached by means of both low interaction energies (low negative values) and low receptor distortion energies (low positive values). In general, the α_{1d}/α_{1b} selective compounds show higher interaction energies and higher distortion energies when they interact with the α_{1b}-AR than with the α_{1d}-AR. The highest affinity towards the α_{1b}-AR is shown by compound **7** and is associated with the lowest α_{1b}-AR distortion energy. As for the α_{1a}-AR subtype, the highest affinity

values are associated with low interaction energies and low receptor distortion energies.

Structural features of ligand–receptor selective interaction

The drawings shown in Figure 1 may give a general idea about how the considered antagonists are oriented into the binding sites of the three α_1-AR subtypes. In general, the protonated nitrogen atom of all the antagonists makes charge reinforced H-bonding interaction with the carboxylate of D3:07 (the first digit indicates the helix and the last two digits indicate the position of the residue in the helix), whereas the other molecular moieties fit two binding pockets formed by TM1, TM2, and TM7 on one side, and by TM4, TM5, and TM6 on the other one, lying in an almost symmetrical topography with respect to D3:07. The α_1-AR antagonists usually are constituted by two aromatic moieties on the two sides of the protonated nitrogen atom. In the proposed interaction models, the aromatic moiety closer to the protonated
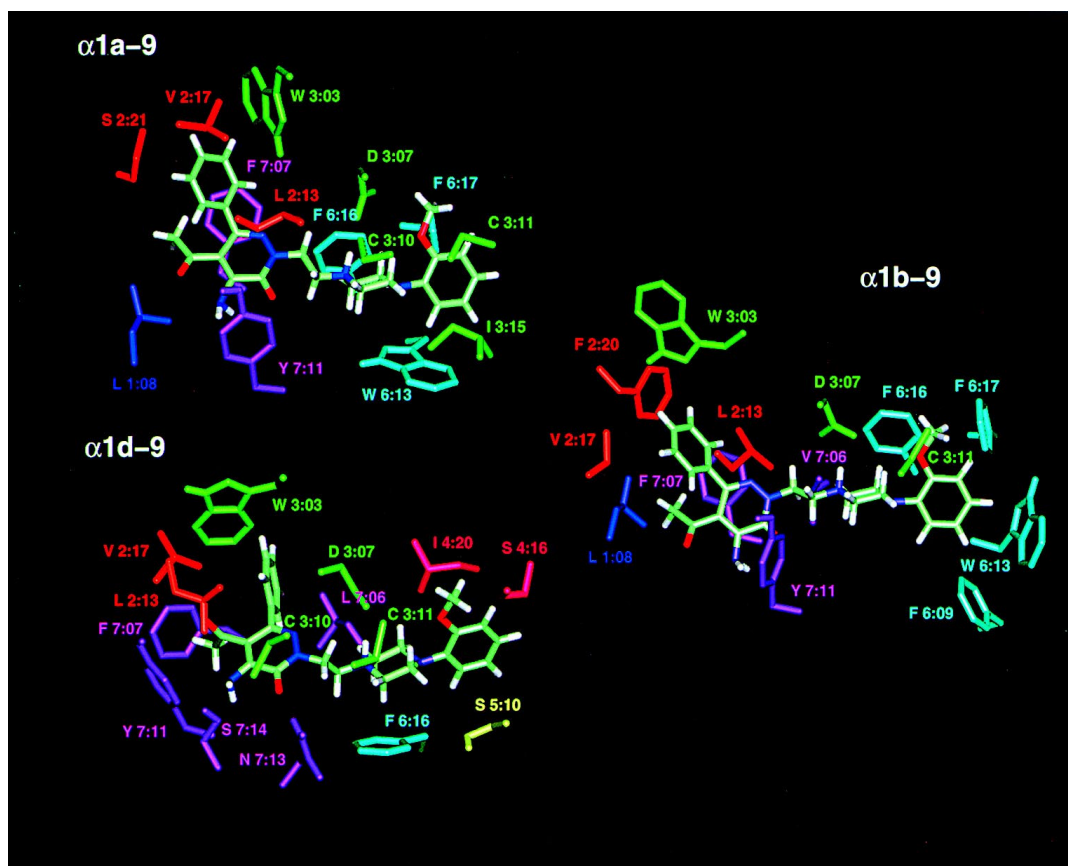

Figure 1. Details of the interaction between compound **9** and the three α_1-AR subtypes. The antagonist–receptor complexes are viewed from the intracellular side of the membrane in a direction parallel to the helix main axes. Residues are labeled according to an arbitrary numbering: the first digit indicates the helix and the last two digits indicate the position of the residue in the helix. Helices **1**, **2**, **3**, **4**, **5**, **6** and **7** are colored in blue, orange, green, pink, yellow, light blue and violet, respectively.

nitrogen atom docks into the hydrophobic pocket formed by residues of TM4, TM5, and TM6.

Interestingly, as clearly shown by Figure 2, the 4,5,6-trisubstituted-3-(2*H*)-pyridazinones and the corresponding 3,4-disubstituted-isoxazolo-[3,4-*d*]-pyridazin-7-(6*H*)-ones give quite similar interaction patterns with each of the three α_1-AR subtypes, which is consistent with their having similar binding affinity profiles. Similarly, the addition of a chlorine atom in the 5-position of the 2-methoxyphenylpiperazine moieties of compounds **5** and **9**, giving the derivatives **6** and **10**, respectively, does not add any change in their interaction patterns.

On the contrary, the lengthening (i.e., **11**) or the shortening (i.e., **4** and **8**) of the spacer even if by a single methylenic unit, causes dramatic differences in the interaction mechanisms in comparison with the corresponding ethylenic derivatives (i.e., **5**, **6**, **9**, and **10**). In particular, as for compound **11**, the lengthening of the ethylenic spacer into a propylenic chain induces not

only a change in the interaction pattern involving the 4,5,6-trisubstituted-3-(2*H*)-pyridazinone moiety and the aromatic cluster formed by W3:03, F7:07 and Y7:11, but also the geometry of the charge reinforced H-bonding interaction between the protonated nitrogen atom of the ligand and the carboxylate side chain of D3:07 and, hence, the orientation of the phenyl-piperazine. Moreover, the shortening of the spacer of compounds **5** and **9** into a methylenic chain induces the 3,4-disubstituted-isoxazolo-[3,4-*d*]-pyridazin-7-(6*H*)-one and the 4,5,6-trisubstituted-3-(2*H*)-pyridazinone moieties of compounds **4** and **8**, respectively, to interfere with the interaction between the protonated nitrogen atom of the ligands and D3:07 of the receptor (Figure 2). As a consequence, the **4**- and **8**-α_{1d} receptor complexes show higher interaction energies and higher receptor distortion energies than the corresponding homo-derivatives **5** and **9**, which is consistent with their having affinity profiles. As shown by Figure 2, the two compounds **4** and **8** give a very similar interaction pattern, which is consistent with their having binding affinity profiles.
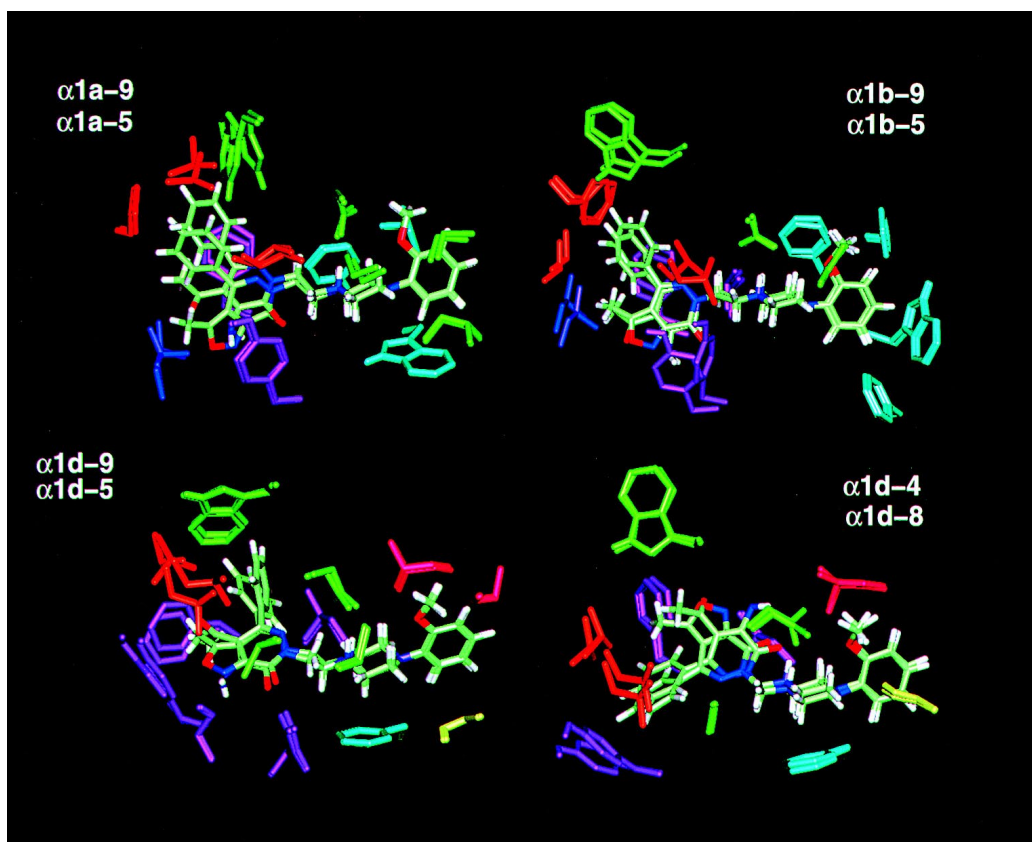

Figure 2. Details of the interaction between compounds **9** and **5** and the three α_1-AR subtypes. The complexes between compound **9** and each of the three α_1-AR subtypes have been superimposed to those between compound **5** and the corresponding α_1-AR subtype. Moreover, in the bottom right side of this figure, the superimposed complexes between compounds **4** and **8** and the α_{1d}-AR subtype are also represented.

In summary, among the new synthesized compounds, the most interesting derivatives carry an ethylenic spacer between the protonated 2-methoxyphenylpiperazine or the 2-methoxy-5-chloro-phenyl-piperazine and the 4,5,6-trisubstituted-3-(2H)-pyridazinone or the 3,4-disubstituted-isoxazolo-[3,4-d]-pyridazin-7-(6H)-one moieties. In fact, these antagonists show slight α_{1d}/α_{1a}, high α_{1d}/α_{1b}, and very high $\alpha_{1a}/5$-HT$_{1A}$ and $\alpha_{1d}/5$-HT$_{1A}$ selectivities. The ethylenic spacer serves to place the 4,5,6-trisubstituted-3-(2H)-pyridazinone or the 3,4-disubstituted-isoxazolo-[3,4-d]-pyridazin-7-(6H)-one moieties into a hydrophobic pocket mainly formed by residues of TM1, TM2, and TM7 in such a way that, as for the α_{1a} subtype, the pyridazinone moiety and the substituent phenyl ring form a π–π sandwich interaction with F7:07 and Y7:11 and an orthogonal σ–π interaction with W3:03, respectively, while as for the α_{1d} subtype, the pyridazinonic carbonylic oxygen atom forms an H-bonding interaction with N7:13 and the substituent phenyl ring forms orthogonal σ–π interactions with both W3:03 and F7:07 (Figure 2). These interactions together with the van der Waals attractive interactions with L2:13 and V2:20 might contribute to the stronger interaction energies and the lower distortion energy shown by **5**, **6**, **9**, and **10** when they interact with both the α_{1a} and the α_{1d}-AR subtypes rather than with the α_{1b} subtype. Interestingly, the protonated nitrogen atom of these compounds gives the strongest charge reinforced H-bonding interactions with the carboxylate ion of D3:07 in the α_1d subtypes with respect to the other two subtypes.

Either selective or nonselective compounds give different interaction patterns when they bind to the three α_1-AR subtypes. This is mainly due to the fact that the ligand binding site of these subtypes, even if constituted by conserved residues, have different structural/dynamics features as a consequence of the intramolecular influence exerted by the non-conserved residues.

Very recently, experimental evidences have emerged which support our hypothesis that the three α_1-AR subtypes have different structural/dynamics behavior and that, in particular, the α_{1a}-AR subtype is more flexible and more sensitive to the environmental conditions with respect to the other two subtypes.[30]

Conclusion

The new compounds presented in this work show, in general, a very good selectivity between the α_1-adrenoceptor and the 5-HT$_{1A}$ serotonergic receptor. Moreover, four of them (**5**, **6**, **9**, and **10**) are provided with remarkable α_{1d}/α_{1b} and a slight α_{1d}/α_{1a}-selectivity.

Taken together, these results suggest that the new N-arylalkylpiperazines can be considered good templates for the development of novel α_{1d} selective ligands, with respect to both of the other two α_1-AR subtypes and the 5-HT$_{1A}$ serotonergic receptor. The importance of such compounds is remarkable, considering that the development of high affinity and selective antagonists for the α_{1d}- or the α_{1b}-subtypes is quite difficult. In fact, BMY 7378, one of the few known α_{1d}-selective antagonists, with respect to the two other AR-subtypes, binds also the 5-HT$_{1A}$ receptor with nanomolar affinity.

Finally, the computational simulated interaction between the new synthesized compounds and the three α_1-AR subtypes confirms our previous hypothesis that selective and nonselective antagonists give different interaction patterns when they bind the three α_1-AR subtypes.[23] This is mainly due to the fact that the ligand binding sites of these subtypes, even if constituted by conserved residues, have different structural/dynamics features as a consequence of the intramolecular influence exerted by the nonconserved residues.

Experimental

Chemistry

Melting points were determined on a Büchi 510 capillary melting points apparatus and are uncorrected. Elemental analyses for the test compounds were within ± 0.4% of the theoretical values. ^{1}H NMR spectra were recorded on a Brüker AC200 spectrometer; chemical shifts are reported as δ (ppm) relative to tetramethylsilane as internal standard. CDCl$_3$ was used as the solvent, unless otherwise noted. TLC on silica gel plates was used to check product purity. Silica gel 60 (Merck; 70–230 mesh) was used for column chromatography and silica gel 60 (Merck, 230–400 mesh) for flash chromatography. The structures of all compounds were consistent with their analytical and spectroscopic data.

3-Methyl-4-phenyl-6-[(4-substitutedphenylpiperazin-1-yl) alkyl]-isoxazolo-[3,4-d]-pyridazin-7-(6H)-ones (5–7): General methods. Method A. (a) A mixture of **1** (1 mmol), the required dibromoalkane (10 mmol) and K$_2$CO$_3$ (1.5 mmol) in DMF (8 mL) was stirred at rt for 5 h. The mixture was then poured into water (15 mL) and extracted with dicloromethane (3×10 mL). After drying and evaporation of the solvent, the residue was normally used as such for the next step. When necessary, it could be purified by silica gel chromatography, eluting with cyclohexane:EtAc (8:2). (b) A mixture of the required bromoalkylpyridazinone (1 mmol), the appropriate phenylpiperazine (1.5 mmol) and K$_2$CO$_3$

(1.5 mmol) in acetone (20 mL) was refluxed overnight. After cooling, the inorganic salts were filtered off and the residue purified by silica gel chromatography, eluting with $CH_2Cl_2/MeOH$ 98/2. See Scheme 1 and Table 1 for data.

Method B. A mixture of **1** (1 mmol), K_2CO_3 (1.5 mmol) and the required chloroalkylphenylpiperazine (1.5 mmol) in acetone (20 mL) was refluxed overnight. After cooling, the inorganic salts were filtered off, the solvent evaporated under vacuum and the residue purified by silica gel chromatography eluting with CH_2Cl_2:EtAc (4:6). See Scheme 2 and Table 1 for data.

4-Amino-5-acetyl-6-phenyl-2-[(4-substitutedphenylpiper-azin-1-yl)alkyl]-3(2H)-pyridazinones (9–11): General method. Compounds were prepared according to the above reported methods A and B, starting from **2**. See Table 1 for data.

3-Methyl-4-phenyl-6-[(4-*ortho*-methoxyphenylpiperazin-1-yl)methyl]-isoxazolo-[3,4-*d*]-pyridazin-7-(6H)-one (4). A mixture of **1** (0.1 g, 0.44 mmol), 37% formaldehyde (1.7 mL, 0.44 mmol) and *ortho*-methoxyphenylpiper-azine (0.13 g; 0.67 mmol) in EtOH (6 mL) was refluxed for 2 h. After cooling and concentration of the solvent, the so formed precipitate was filtered to give 0.15 g (79%) of **4**, mp 166–168 °C (see also Table 1)

4-Amino-5-acetyl-6-phenyl-2-[(4-*ortho*-methoxyphenyl-piperazin-1-yl)methyl]-3(2H)-pyridazinone (8). Compound was prepared as above reported for **4**, starting from **2**. Yield 83%, mp 198–200 °C (see also Table 1).

4-Phenyl-6-methyl-3-[(4-*ortho*-methoxyphenylpiperazin-1-yl)methyl]-isoxazolo-[3,4-*d*]-pyridazin-7-(6H)-one (12). A solution of **3*** (0.2 g, 0.6 mmol) and *ortho*-methoxy-phenylpiperazine (0.32 g, 1.6 mmol) in $CHCl_3$ (6 mL) was refluxed for 2 h. After cooling and evaporation of the solvent, the residue was purified by flash chromatography eluting with cyclohexane:EtAc (8:2). Yield 79%, mp 177–178 °C. ^1H NMR: δ 2.4–2.5 (m, 4H), 2.9–3.0 (m, 4H), 3.7 (s, 2H), 3.8 (2s, 6H), 6.9–7.0 (m, 4H), 7.5–7.7 (m, 5H). $C_{23}H_{25}N_5O_3$ (C,H,N)

2-Methyl-4-amino-6-phenyl-5-[(4-ortho-methoxyphenyl-piperazin-1-yl)acetyl]-3(2H)-pyridazinone (13). A mixture of **12** (0.08 g, 0.00018 mol), hydrazine hydrate (0.04 mL, 0.0007 mol) and 10% Pd-C (0.02 g) in EtOH (5 mL) was refluxed for 1 h. The still-hot mixture was filtered, the catalyst thoroughly washed with CH_2Cl_2, the solvent evaporated and the residue purified by silica gel chro-matography, eluting with CH_2Cl_2:MeOH (98:2). Yield 30%. ^1H NMR: δ 2.7–2.8 (m, 2H), 3.0–3.2 (m, 4H), 3.4–3.5 (m, 2H), 3.7–3.8 (app. d., 6H), 6.9–7.0 (m, 6H), 7.5–7.7 (m, 5H). $C_{23}H_{27}N_5O_3$ (C,H,N).

Radioligand binding assays at native receptors. Binding studies on native α_1 adrenergic and 5-HT$_{1A}$ serotonergic receptors were carried out in membranes of rat cerebral cortex (α_1) and hippocampus (5-HT$_{1A}$). Male Sprague–Dawley rats (200–300 g, Charles River, Italy) were killed by cervical dislocation and different tissues were excised and immediately frozen and stored at −70 °C until use. Tissues were homogenized (2×20 s) in 50 vols of cold Tris–HCl buffer pH 7.4, using a Politron homogenizer (speed 7). Homogenates were centrifuged at 49000g for 10 min, resuspended in 50 vols of the same buffer, incubated at 37 °C for 15 min and centrifuged and resuspended twice more. The final pellets were suspended in 100 vols of Tris–HCl buffer pH 7.4, containing 10 μM pargiline and 0.1% ascorbic acid. Membranes were incubated in a final volume of 1 mL for 30 min at 25 °C with 0.1–0.5 nM [^{3}H]prazosin (α_1) or 0.5–1.5 nM [^{3}H]8-OH-DPAT (5-HT$_{1A}$), in absence or presence of competing drugs; nonspecific binding was determined in the presence of 10 μM phentolamine (α_1), or 10 μM 5-HT (5-HT$_{1A}$).

The incubation was stopped by addition of ice-cold Tris–HCl buffer and rapid filtration through 0.2% polyethyleneimine pretreated Whatman GF/B or Schleicher & Schuell GF52 filters. The filters were then washed with ice-cold buffer and the radioactivity retained on the filters was counted by liquid scintillation spectrometry.

Radioligand binding assay at cloned α_1-adrenoceptors. Binding to cloned human α_1-adrenoceptor subtypes was performed in membranes from CHO cells (Chinese hamster ovary cells) transfected by electroporation with DNA expressing the gene encoding each α_1-adreno-ceptor subtype. Cloning and stable expression of the human α_1-adrenoceptor gene was performed as previously described.[9] CHO cell membranes (30 μg proteins) were incubated in 50 mM Tris–HCl, pH 7.4, with 0.1–0.4 nM [^{3}H]prazosin, in a final volume of 1 mL for 30 min at 25 °C, in absence or presence of competing drugs (1 pM–10 μM). Nonspecific binding was determined in the presence of 10 μM phentolamine. The incubation was stopped by addition of ice-cold Tris–HCl buffer and rapid filtration through 0.2% poly-ethyleneimine pretreated Whatman GF/B or Schleicher & Schuell GF52 filters.

Data analysis

The inhibition of specific binding of the radioligands by the tested drugs was analyzed to estimate the IC$_{50}$ value by using the nonlinear curve-fitting program Allfit.[31] The IC$_{50}$ value is converted to an affinity constant (K_i) by the equation of Cheng and Prusoff.[32]

Modeling

3D Model building of the α_1-AR subtypes and docking simulations. The building of the transmembrane (TM) model of the three-α_1-AR subtypes was described in detail in our previous papers.[23,33] The input structures of the ligand–receptor complexes were obtained by docking each ligand into the target receptor structure averaged over the last 100 picoseconds of the Molecular Dynamics simulation. For each complex several minimizations were performed in order to probe different orientations and conformations of the ligands and to optimize several fundamental interactions (i.e., the charge reinforced H-bond between the protonated nitrogen atom of the ligands and the carboxylate of D3:07), which is the putative key residue for the cationic ligand-receptor recognition.[34]

Modeling studies were performed with the molecular graphics package QUANTA (version 4.0).[35] Energy minimizations and MD simulations were obtained by means of the program CHARMm (version 22).[36] Minimizations were carried out by using 200 steps of steepest descent followed by a conjugate gradient minimization, until the rms gradient was less than 0.001 kcal/mol Å. A distance dependent dielectric term ($\varepsilon = 4r$) and a 12 Å nonbonded cutoff distance were chosen. The 'united atom approximation' was used for computational efficiency.[36] The charge distributions of the ligands in their protonated form were obtained in the AM1 framework.[37]

References and Notes

1. Morrow, A. L.; Creese, I. *Mol. Pharmacol.* **1986**, *29*, 321.

2. Han, C.; Abel, P. V.; Minneman, K. P. *Nature* (London) **1987**, *329*, 333.

3. Hanft, G.; Gross, G. *Br. J. Pharmacol.* **1989**, *97*, 691.

4. Boer R.; Grassegger, A.; Schudt, C. H.; Glossman, H. *Eur. J. Pharmacol.* **1989**, *172*, 131.

5. Cotecchia, S.; Schwinn, D. A.; Randall, L. L.; Lefkowitz, R. J.; Caron, M. G.; Kobilka, B. K. *Proc. Natl. Acad. Sci. U.S.A.* **1988**, *85*, 7159.

6. Schwinn, D. A.; Lomasney, J. W.; Lorenz, W.; Szklut, P. J.; Fremeau, R. T.; Yang-Feng, T. L.; Caron, M. G.; Lefkowitz, R. J.; Cotecchia, S. *J. Biol. Chem.* **1990**, *265*, 8183.

7. Lomasney, J. W.; Cotecchia, S.; Lorenz, S.; Leung, W.; Schwinn, D. A; Yang-Feng, T. L.; Brownstein, M.; Lefkowitz, R. J.; Caron, M. G. *J. Biol. Chem.* **1991**, *266*, 6365.

8. Perez, D. M.; Piascik, M. T.; Graham, R. M. *Mol. Pharmacol.* **1991**, *40*, 876.

9. Schwinn, D. A.; Lomasney, J. W. *Eur. J. Pharmacol.* **1992**, *227*, 433.

10. Laz, T. M.; Forray, C.; Smith, K. E.; Bard, J. A.; Vaysse, P. J. J.; Branchek, T. A.; Weinshank, R. L. *Mol. Pharmacol.* **1994**, *46*, 414.

11. Forray, C.; Bard, J. A.; Wetzel, J. M.; Chiu, G.; Shapiro, E.; Tang, R.; Lepor, H.; Hartig P. R.; Weinshank, R. L.; Branchek, T. A.; Gluchowski, C. *Mol. Pharmacol.* **1994**, *45*, 703.

12. Forray, C.; Bard, J. A.; Laz, T. M.; Smith, K. E.; Vaysse, P. J.; Weinshank, R. L.; Gluchowski, C.; Branchek, T. A. *Faseb J.* **1994**, *8*, A353.

13. Hieble, J. P.; Bylund, D. B.; Clarke, A. E.; Eikenberg, D. C.; Langer, S. Z.; Lefkowitz, R. J.; Minneman, K. P.; Ruffolo, R. R. *Pharmacol. Rev.* **1995**, *47*, 267.

14. Ford, A. P. D. W.; Williams, T. J.; Blue, D. R.; Clarke, D. E. *Trends Pharmacol. Sci.* **1994**, *15*, 167.

15. Testa, R.; Taddei, C.; Poggesi, E.; De Stefani, C.; Cotecchia, S.; Hieble, J. P.; Sulpizio, A. C.; Naselsky, D. P.; Bergsma, D. J.; Ellis, C.; Swift, A.; Ganguly, S.; Ruffolo, R. R. Jr.; Leonardi, A. *Pharmacol. Comm.* **1995**, *6*, 79.

16. Pimoule, C.; Langer, S.; Graham, D. *Eur. J. Pharmacol-Mol. Pharmacol.* **1995**, *290*, 49.

17. Schwinn, D. A.; Johnston, G. I.; Page, S. O.; Mosley, M. J.; Wilson, K. H.; Worman, N. P.; Campbell, S.; Fidock, M. D.; Furness, L. M.; Parry-Smith, D. J.; Peter, B.; Bailey, D. S. *J. Pharmacol. Exp. Ther.* **1995**, *272*, 134.

18. Goetz, A. S.; King, H. K.; Ward, S. D. C.; True, T. A.; Rimele, T. J.; Saussy, D. L. Jr. *Eur. J. Pharmacol.* **1995**, *272*, R5.

19. Hieble, J. P.; Ruffolo, R. R. Jr.; Sulpizio, A. C.; Naselsky, D. P.; Conway, T. M.; Ellis, C.; Swift, A. M.; Ganguly, S.; Bergsma, D. *J. Pharmacol. Comm.* **1995**, *6*, 91.

20. Flavahan, N. A.; Vanhoutte, P. M. *Trends Pharmacol. Sci.* **1986**, *7*, 347.

21. Muramatsu, I.; Ohmura, T.; Kigoshi, S.; Hashimoto, S.; Oshita, M. *Br. J. Pharmacol.* **1990**, *99*, 197.

22. Muramatsu, I.; Ohmura, T.; Hashimoto, S.; Oshita, M. *Pharmacol. Comm.* **1995**, *6*, 23.

23. De Benedetti, P. G.; Fanelli, F.; Menziani, M. C.; Cocchi, M.; Testa, R; Leonardi, A. *Bioorg. Med. Chem.* **1997**, *5*, 809.

24. Montesano, F.; Barlocco, D.; Cignarella, G.; De Benedetti, P. G.; Fanelli, F.; Leonardi, A.; Taddei, C. *5th International Symposium on the Chemistry and Pharmacology of Pyridazines, Sopron (Hungary)*, 1996, P13.

25. Sprio, V.; Aiello, E.; Mazza, A. *Annali di Chimica,* **1967**, *57*, 836.

26. Romeo, G.; Russo, F.; Guccione, S.; Barbarulo, D.; De Blasi, A. *Il Farmaco* **1995**, *50*, 471.

27. Amschler, H.; Krastinat, W. *Ger. Offen. 2,258,561; Chem. Abstr.* **1973**, *79*, 78841a.

28. Dal Piaz, V. Personal communication.

29. Leonardi, A.; Testa, R.; Motta, G.; De Benedetti, P. G.; Hieble, P.; Giardina', D. In *Perspective in Receptor Research*; Giardina', D.; Piergentili, A.; Pigini, M., Eds; Elsevier Science B.V.: Amsterdam, 1995; p 135.

30. Ford, A. P. D. W; Daniels, D. V.; Chang, D. J.; Diaz, M. R.; Gever, J. R.; Jasper, J. R.; Lesnick, J. D.; Clarke, D. E. *Brit. J. Pharmacol.* **1996**, *118*, 29P.

31. DeLean, A.; Munson, P. J.; Rodbard, D. *Am. J. Physiol.* **1978**, *235*, E97.

32. Cheng, Y. C.; Prusoff, W. H. *Biochem. Pharmacol.* **1973**, *22*, 3099.

33. Fanelli, F.; Menziani, M. C.; Cocchi, M.; De Benedetti, P. G. *J. Mol. Struct. (Theochem)* **1995**, *333*, 49.

34. Cavalli, A.; Fanelli, F.; Taddei, C.; De Benedetti, P. G.; Cotecchia, S. *FEBS Lett.* **1996**, *399*, 9.

35. Quanta/CHARMm, *1990 Molecular Simulations, 200 Fifth Avenue.*

36. Brooks, B. R.; Bruccoleri, R. E.; Olafson, B. D.; States, D. J.; Swaminathan, S.; Karplus, M. *J. Comput. Chem.* **1983**, *4*, 187.

37. Dewar, M. J. S.; Zoebisch, E. G.; Healey, E. F.; Stewart, J. J. P. *J. Am. Chem. Soc.* **1985**, *107*, 3902.